

Molecular Dynamics Simulations of CO₂ Formation in Interstellar Ices

C. Arasa,^{†,‡} M. C. van Hemert,[†] E. F. van Dishoeck,[‡] and G. J. Kroes^{*,†}

Gorlaeus Laboratories, Leiden Institute of Chemistry, Leiden University, P. O. Box 9502, 2300

RA Leiden, The Netherlands, and Leiden Observatory, Leiden University, P. O. Box 9513, 2300

RA Leiden, The Netherlands

E-mail: g.j.kroes@chem.leidenuniv.nl

Abstract

CO₂ ice is one of the most abundant components in ice-coated interstellar ices besides H₂O and CO, but the most favorable path to CO₂ ice is still unclear. Molecular dynamics calculations on the ultraviolet photodissociation of different kinds of CO–H₂O ice systems have been performed at 10 K in order to demonstrate that the reaction between CO and an OH molecule resulting from H₂O photodissociation through the first excited state is a possible route to form CO₂ ice. However, our calculations, which take into account different ice surface models, suggest that there is another product with a higher formation probability $((3.00 \pm 0.07) \times 10^{-2})$, which is the HOCO complex, whereas the formation of CO₂ has a probability of only $(3.6 \pm 0.7) \times 10^{-4}$. The initial location of the CO is key to obtain reaction and form CO₂: the CO needs to be located deep into the ice. The HOCO complex becomes trapped in the cold ice surface in the *trans*-HOCO minimum because it quickly loses its internal energy

*To whom correspondence should be addressed

[†]Gorlaeus Laboratories, Leiden Institute of Chemistry, Leiden University, P. O. Box 9502, 2300 RA Leiden, The Netherlands

[‡]Leiden Observatory, Leiden University, P. O. Box 9513, 2300 RA Leiden, The Netherlands

to the surrounding ice, preventing further reaction to $\text{H} + \text{CO}_2$. Several laboratory experiments have been carried out recently and they confirm that CO_2 can also be formed through other, different routes. Here we compare our theoretical results with the data available from experiments studying the formation of CO_2 through a similar pathway as ours, even though the initial conditions were not exactly the same. Our results also show that the HCO van der Waals complex can be formed through the interaction of CO with the H atom that is formed as a product of H_2O photodissociation. Thus, the reaction of the H atom photofragment following H_2O photodissociation with CO can be a possible route to form HCO ice.

Keywords: molecular dynamics – water ice – CO_2 ice – interstellar medium

Introduction

In cold and dense regions of interstellar clouds where new stars are formed several molecules have been observed in the solid state, such as H_2O , CO, CO_2 , NH_3 , CH_4 , and CH_3OH (among others).^{1,2} Interstellar CO_2 ice has been detected for the first time in 1989 by d’Hendecourt and de Muizon,³ confirmed by de Graauw *et al.*,⁴ and it has been observed along many lines of sight with a constant $\text{CO}_2/\text{H}_2\text{O}$ abundance ratio of about 0.3, with a high column density.⁵ The large amounts of CO_2 ice observed cannot be explained by gas-phase reactions,⁶ and also because of the large amount of solid CO found in ice,⁷ it is believed that CO_2 must be formed through solid phase reactions. However, its formation path is not at all understood yet, and in the literature different routes to form CO_2 in ice have been proposed.^{8–18}

Ground state CO can react with an electronically excited CO^* molecule leading to CO_2 and atomic C. This reaction has been studied experimentally in different laboratories.^{8–10} CO_2 can also be formed after irradiating CO ice with $\text{Ly}\alpha$ photons, and subsequently bombarding the ice with energetic protons of 200 keV,⁸ or by irradiating the CO ice with 5 keV electrons in order to simulate the effect of cosmic ray particles, thereby breaking the CO bond and creating energetic atomic O.^{9,10}

Another possible path to form ground state CO_2 is by the reaction between CO with atomic $\text{O}(^3\text{P})$. Roser *et al.*¹¹ and Madzunkov *et al.*¹² demonstrated that this is a possible route to form

CO₂ using temperature programmed desorption (TPD) experiments, in one case using thermal O atoms below 160 K,¹¹ and in another case using energetic O atoms (from 2 to 14 eV)¹² in order to overcome the high reaction barrier.¹⁹ However, Grim *et al.*¹⁹ demonstrated that the reaction CO(¹Σ) + O(³P) → CO₂ does not take place on cold grain surfaces (10–20 K) due to its high activation energy (2970 K in the gas-phase²⁰).

A third mechanism is based on the reaction CO + OH → CO₂ + H, where the OH can result either from H₂O photodissociation (the photolysis mechanism) or thermal hydrogenation of oxygen species (the hydrogenation mechanism). Recent laboratory experiments show that both routes are efficient at low ice temperatures (10–20 K).^{13–18} In 2002, Watanabe *et al.*¹³ measured the conversion rates of CO to CO₂ irradiating the ice with photons with an energy close to Lyα, using H₂O and D₂O mixed with CO ices (with a ratio of H₂O/CO ≈ 10) at 12 K and a photon flux of the order of 10¹⁴–10¹⁵ photons s⁻¹ cm⁻². After two hours irradiation time, corresponding to a photon dose of about 10¹⁸ photons cm⁻², most of the CO is converted to CO₂ with a rate constant of about 2.5 × 10⁻⁴ s⁻¹ as obtained from fits of Fourier transform infrared spectroscopy (FTIR) measurements. They concluded that the rate constant is very small and suggested that CO is not immediately converted to CO₂, probably because some intermediate like HOCO or DOCO is formed first. They did not detect HOCO, but in the end, over the long timescales of hours in the experiment, this may lead to CO₂ and hydrogen or deuterium atom, respectively. In these experiments, no isotope effects were observed.

In 2007, Watanabe *et al.*¹⁴ also studied the formation of CO₂ through the hydrogenation mechanism as well as the photolysis mechanism in two types of ices: a CO–H₂O mixture (with a ratio of H₂O/CO ≈ 4), and a pure H₂O ice layer with a total thickness of about 30 monolayers with one monolayer of CO on top at low ice temperatures (10–50 K). The measured photon flux was 5.9 × 10¹³ photons s⁻¹ cm⁻² with an energy in the range of the Lyman band and close to Lyα. After irradiating the ices for two hours, several products were identified in the spectra, such as CO₂, which was the most abundant product, but also HCOOH, H₂CO, CH₃OH, as well as HCO and CH₃CHO, the presence of which was inferred from small peaks. The CO₂ was assumed to be formed from the reaction of CO with OH, because CO cannot be dissociated at the UV photons energies used in these experiments. The experimentalists also

fitted their data to a kinetic model in order to calculate the rate constants to form CO₂, H₂CO, and HCOOH from CO, based on the column densities of these photoproducts and assuming that H₂O is constantly dissociated. According to their analysis, CO is converted to CO₂ with a rate constant of $3.3 \pm 0.17 \times 10^{-4} \text{ s}^{-1}$ at 10 K, in close agreement with the value reported previously by Watanabe *et al.*¹³ However, after the bombardment of the ice with H atoms, HCO was the most abundant product, and also H₂CO and CH₃OH, but no CO₂ was detected in the infrared (IR) absorption spectrum.

Another recent laboratory study on the formation of CO₂ ice through surface reactions of CO molecules with OH radicals formed after H₂O photodissociation was done by Oba *et al.*¹⁵ In these experiments, CO molecules were introduced in the main chamber, and also H₂O molecules that are dissociated by a microwave induced plasma. The experiments were carried out at 10 and 20 K for two hours. During the irradiation time the ratio OH/CO was about 0.8, and the products were recorded by infrared reflection absorption spectroscopy (RAIRS). From the IR spectra some lines were assigned to the following products: CO₂, H₂CO₃, and *trans*-HOCO and *cis*-HOCO, which disappear at higher temperatures. The experimentalists concluded that CO₂ is formed by reaction of the OH radicals (that have low energies) with the CO matrix at low temperatures (below 20 K). However, it is expected that at higher temperatures the OH has enough energy to migrate far away from the CO, and the reaction may not be feasible.

In a different kind of experiments, Ioppolo *et al.*¹⁶ deposited a mixture of CO:O₂ ice on a substrate at low temperatures (15 and 20 K) and bombarded the ice with a cold H atom beam, leading to the formation of thermal OH radicals, which after long timescales in the end reacted with CO to form CO₂. The products formed in the ice were monitored by means of RAIRS. Noble *et al.*¹⁷ studied the formation of CO₂ ice in a nonporous H₂O ice and on an amorphous silicate surface through the reaction of CO with OH, where the OH radicals were formed after the hydrogenation of O₂ and O₃, and the formation of CO₂ in ice was demonstrated by means of TPD experiments. Zins *et al.*¹⁸ also studied the reactivity between CO and OH molecules at very low temperatures (3.5 K). The OH radicals were formed from discharged H₂O/He mixtures and they were mixed with a mixture of CO and CO₂. A Fourier transform infrared

spectrometer was used in order to monitor all the products that were formed in the ice, such as CO₂, H₂CO, H₂O, and HO₂, among others. The formation of the HOCO complex was also observed when the OH radicals and the CO molecules were injected at the same time, as an intermediate to the formation of CO₂.

Here the photo-induced pathway is studied, building on our previous molecular dynamics (MD) simulations of the photodissociation of water molecules in crystalline and amorphous water ice²¹⁻²³ in order to better understand the formation of CO₂ through the reaction between CO and OH from a fundamental molecular physics point of view. We also wanted to prove that CO₂ can indeed be formed through this route even though the system has to pass through a deep well (the HOCO well) on the way to the exit channel barrier to reaction, so that the system could be trapped in the well if the energy of HOCO is efficiently dissipated to the surrounding ice. In our simulations, the OH + CO reaction is based on the gas-phase potential energy surface developed by Lakin *et al.*²⁴ that gives rise to low cross section values for the gas-phase reactions²⁵⁻²⁷ due to the barriers that the system has to overcome in order to eventually form CO₂ and H as is described later. However, in our simulations the OH radical formed after H₂O photodissociation in many cases comes off vibrationally excited, and this might enhance the formation of CO₂ compared to the gas-phase case.

We report results for MD simulations on the photoinduced reaction of the photofragment OH radical with CO in different kinds of CO-H₂O ice conditions at 10 K, where a single H₂O molecule is photodissociated by a single photon. This low flux simulates the flux of UV photons that irradiate ice-coated grains deep inside interstellar clouds, which is of the order of 10³ photons cm⁻² s⁻¹,²⁸⁻³⁰ meaning one incident photon per month per grain, and therefore a photodissociation event will be finished by the time the next photon arrives.

The methods employed in this study are explained in **Methods**, the main results are presented in **Results and discussion**, and the final conclusions are given in **Summary and Conclusion**.

Methods

Classical MD methods³¹ and analytical potentials based on pair potential interactions have been used in order to describe the evolution of the interactions of all the molecules and fragments in a CO–H₂O ice system before and after the absorption of an UV photon by one of the H₂O molecules from the ice. All the specifics of the potentials and the switching functions are presented in the supporting material.³²

Potentials

The total analytical potential energy surface (PES) for the CO–H₂O ice system used to describe the photodissociation of one of the water molecules and the subsequent interaction of the fragments with CO and the other H₂O molecules can be written as follows:

$$V_{\text{tot}} = V_{\text{ice}} + V_{\text{H}_2\text{O}^*-\text{H}_2\text{O}} + V_{\text{H}_2\text{O}^*-\text{CO}} + V_{\text{H}_2\text{O}^*} \quad (1)$$

where

$$V_{\text{ice}} = V_{\text{H}_2\text{O}-\text{H}_2\text{O}} + V_{\text{H}_2\text{O}-\text{CO}} \quad (2)$$

The first term of the total potential (Eq. 1) is given by Eq. 2, which describes the intermolecular interactions between the H₂O molecules inside the ice excluding the H₂O molecule that is photoexcited (Eq. 2), which are described by the TIP4P potential.³³ Eq. 2 also contains the intermolecular interactions between those H₂O and the CO molecules, where all CO and H₂O molecules are kept rigid, and the CO–CO intermolecular interactions if more than one CO molecule is considered in the system. In this work, as expressed by Eq. 2 only one CO molecule is taken into account, in order to limit the complexity of the total system.

The $V_{\text{H}_2\text{O}-\text{CO}}$ potential is based on pair potentials between H₂O and CO molecules and consists of repulsion, dispersion and electrostatic terms based on CCSD(T) calculations using an AVDZ basis set and applying BSSE corrections for 2500 different configurations. The

charges of the H₂O molecules are the same as those used in the TIP4P potential (H:0.52e, O:0e, and the additional charge site M:-1.04e).³³ For the CO molecule we have used negative charges on C and on O (-0.47e and -0.615e, respectively) and a compensating positive charge at the center of mass.

The second term of the total potential (Eq. 1) contains the intermolecular interactions of the photoexcited molecule, which is treated as fully flexible, with the rigid water molecules by means of a TIP3P-type potential.^{21,22,33} The photoexcited molecule will dissociate into H and OH. Thus, this term also takes into account the $V_{\text{H-H}_2\text{O}}$, $V_{\text{OH-H}_2\text{O}}$ interactions as fully described in our previous studies.^{21,22}

The third term of Eq. 1 covers the interactions between the photoexcited water molecule with CO, and the interactions between H with CO, and OH with CO. The $V_{\text{H}_2\text{O}^*-\text{CO}}$ potential is taken to be the same as for ground state H₂O interacting with CO because the lifetime of the excited water molecule is very short (~ 0.2 fs²¹), leading to H and OH which will interact with CO by means of switching functions based on the OH bond distance as described elsewhere.²¹ For the $V_{\text{H-CO}}$ pair potential we fit an H-CO non reactive potential by using dispersion and repulsive terms (more details in Ref.³²). We have used the well known LTSH potential,²⁴ which is a six dimensional PES, to describe the $V_{\text{OH-CO}}$ interaction.

To smoothly switch the intramolecular interaction of OH from the one valid when it interacts with H₂O to that valid when it interacts with CO, we have used a switching function³⁴ based on the distance between the carbon atom with the oxygen atom of OH (more details can be found in the supporting material³²).

The minimum energy path of the OH + CO reaction according to the LTSH PES is plotted in Fig. 1,²⁴ showing a complex minimum energy path (MEP). In the entrance channel there is the OH-CO van der Waals minimum, followed by a small barrier (~ 0.05 eV relative to the van der Waals minimum, the *trans* HO-CO saddle point) and the *trans*-HOCO well with an energy of about -1.3 eV relative to the gas-phase reactants. From the *trans*-HOCO minimum there are two possible paths that bring the system to the H + CO₂ product. The first path (solid line in Fig. 1) connects the *trans*-HOCO minimum to another minimum (of -1.2 eV), the *cis*-HOCO complex via a *cis-trans* barrier of ~ 0.4 eV relative to the *trans*-HOCO minimum.

From the *cis*-HOCO minimum there is another saddle point (*cis*-H-OCO) with a much higher barrier of about 1.3 eV that connects the *cis*-HOCO complex with the final products. This exit channel barrier has a height of about 0.07 eV relative to the gas-phase reactants. The second MEP (dashed line in Fig. 1) connects the *trans*-HOCO complex with another saddle point (HOCO-HCO₂) with a large barrier of about 1.6 eV that leads to the HCO₂ minimum, and this barrier has a height of about 0.34 eV relative to the gas-phase reactants. Finally, the HCO₂ minimum is connected with the final products through an H-CO₂ stationary point that has an energy of 0.2 eV above the HCO₂ minimum. Moreover, since the LTSH PES gives rise to two minima: HOCO and H + CO₂, their interactions with the H₂O molecules must also be included in the total PES. The interaction between HOCO and H₂O has been taken simply as the sum of the OH-H₂O and the H₂O-CO interactions. However, we fit a new PES to describe the V_{H₂O-CO₂} interactions, consisting of the dispersion, repulsive and electrostatic terms based on CCSD(T)/aug-cc-pVTZ calculations for 174 different configurations.³² The H-H₂O interactions were already described before.^{21,22}

The last term of Eq. 1 describes the intramolecular interactions in the water molecule that is photoexcited to the first excited electronic state of gas-phase H₂O (\tilde{A}^1B_1) by means of the Dobbyn and Knowles PES,³⁵⁻³⁷ which is repulsive and leads to dissociation into H and OH, as has already been explained elsewhere.^{21,22}

Amorphous ice surface

To study the UV photodissociation of H₂O ice in an amorphous CO-H₂O ice system followed by the reaction of OH + CO, we have used two different procedures to construct an amorphous CO-H₂O ice system.

The first procedure of growing an ice surface is based on an ‘hit and stick’ method. First, a CO molecule is set up with center of mass coordinates fixed at the origin ($x, y, z=0$). A water molecule is generated with random position and orientation and it interacts with the CO molecule through the H₂O-CO PES described above. The energy of the H₂O-CO system is minimized by using the simplex algorithm.³⁸ The CO-H₂O ice is grown by a consecutive addition of single H₂O molecules and minimizing the interaction energy which is described by

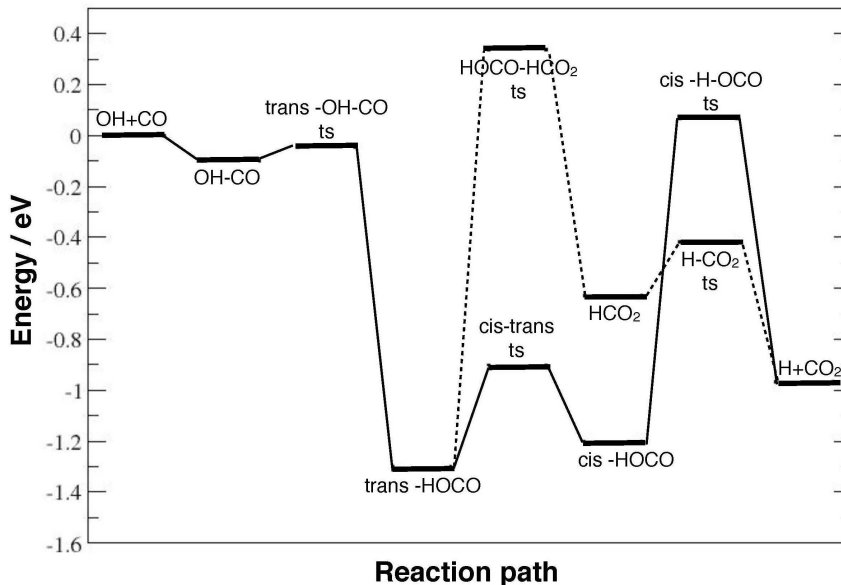


Figure 1: Minimum energy path according to the LTSH potential²⁴ for the reaction $\text{OH} + \text{CO} \leftrightarrow \text{H} + \text{CO}_2$.

the TIP4P PES³³ for the newly arriving H_2O with the H_2O molecules already present in the ice, and by the $\text{H}_2\text{O}-\text{CO}$ PES, using the simplex algorithm. After the amorphous ice is grown it is first thermalized, and next equilibrated at 10 K for 30 ps using MD with a thermostat switched on and off.³⁹ The resulting ice physically looks like an ice ball made up of one CO and 50 H_2O molecules (Fig. 2), and the closest H_2O molecule and the farthest one from the central CO molecule are located at a distance of 3.2 Å, and 7.2 Å, respectively. With this methodology, we have set up three different initial configurations of all the molecules in the ice ball, all of them thermalized at 10 K. The ice balls were used to explore the reactivity in the ice since they require little computer time.

The second procedure is based on our previous amorphous water ice set up.²¹⁻²³ Thus, first a hexagonal crystalline H_2O ice surface was modeled, and from its geometry an amorphous H_2O ice surface was obtained at 10 K using MD simulations³¹ and the fast-quenching method.^{21,40,41} The resulting ice can be divided in 16 monolayers (where the four bottom layers were not allowed to move during the dynamics in order to simulate the bulk), and in total the system contains 480 H_2O molecules with the system described by cell parameters of 22.4 Å,

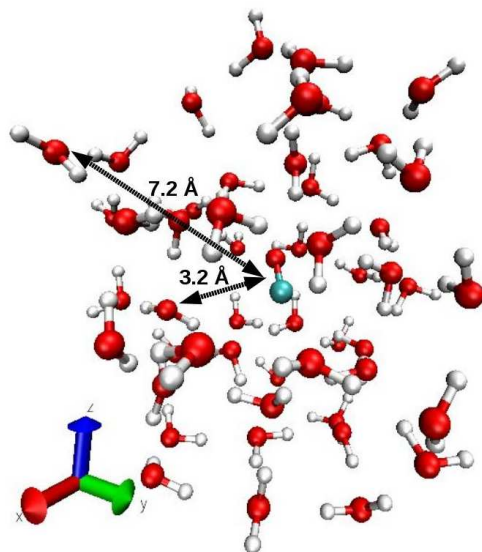


Figure 2: Amorphous ice ball with 50 H₂O molecules and 1 CO molecule in the center. Red balls represent O, white H, and green C atoms.

and 23.5 Å in x and y , respectively.^{21–23} One water molecule was replaced by a CO molecule and its random coordinates and velocities were sampled according to a Maxwell-Boltzmann distribution of 10 K. We considered three different initial scenarios for the CO molecule: it was adsorbed on top of the first monolayer, it was absorbed in the second monolayer of the amorphous water ice surface, or it was absorbed in the fifth monolayer of the amorphous water ice surface. In the three cases, the total system was thermalized at 10 K for 20 ps using a thermostat,³⁹ and later on it was equilibrated for 20 ps using microcanonical ensemble (NVE) MD simulations where the CO–H₂O and H₂O–H₂O interactions were taken into account. In Fig. 3(a), the amorphous CO_{ad}–H₂O ice surface and in Fig. 3(b), and (c), the amorphous CO_{ab}(ML2)–H₂O ice surface and CO_{ab}(ML5)–H₂O ice surface are represented, respectively.

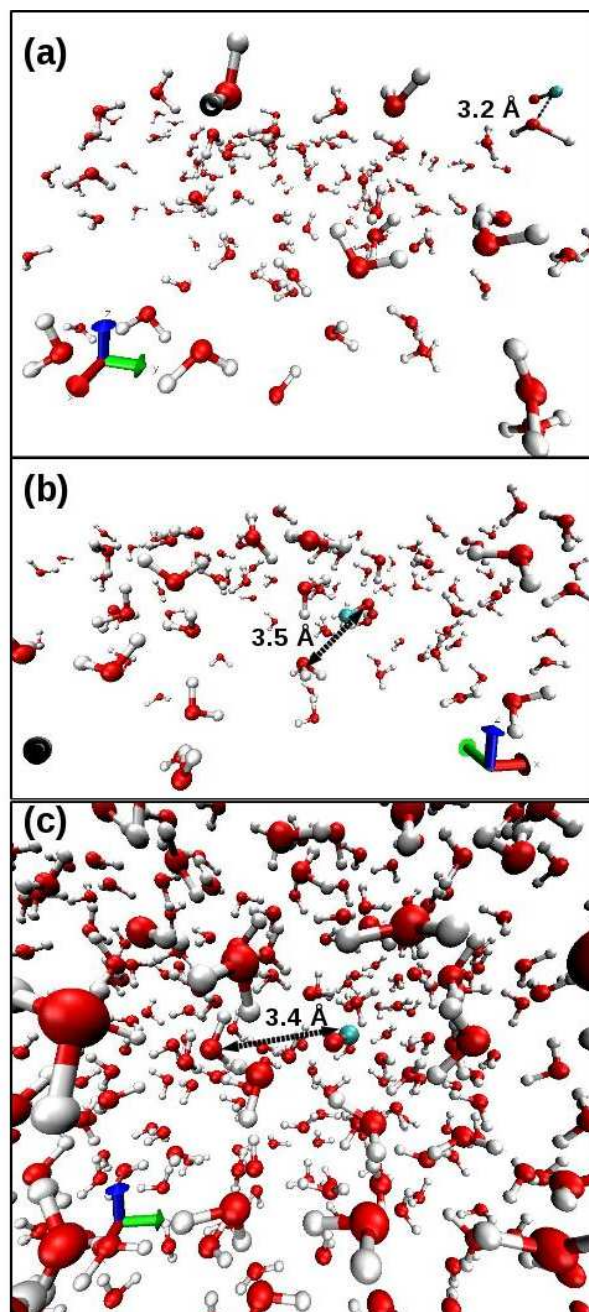


Figure 3: (a) Amorphous ice showing the top four MLs of H₂O and one CO molecule adsorbed on top of ML 1. (b) Amorphous ice showing the top four MLs of H₂O and one CO molecule absorbed in ML 2. (c) Amorphous ice showing twelve MLs of H₂O and one CO molecule absorbed in ML 5. Red balls represent O, white H, and green C atoms.

Initial conditions and dynamics

For both types of CO–H₂O ice surfaces, only the H₂O molecules that are closest to the CO molecule (the distance between the center of mass of CO and the center of mass of water being smaller than 4.5 Å) were selected to be photodissociated, and between 200–2000 different initial coordinates and momenta were generated per excited H₂O molecule. As described elsewhere,^{21–23} in order to initialize the trajectories⁴² a Wigner phase-space distribution function⁴³ fitted to the ground-state vibrational wavefunction of gas-phase water is used. The resulting coordinates and momenta were sampled using a Monte Carlo algorithm, and a vertical excitation is performed to put the system on the first electronically excited state, on the DK \tilde{A}^1B_1 PES.^{35–37} Thus, the molecules are excited with photon energies E_{exc} in the range 7.5–9.5 eV, with a peak at 8.6 eV (see figure 3 in Ref.²¹). From the excitation energy and the dissociation energy of H₂O ($E_{\text{diss}}(\text{H}_2\text{O}) \approx 5.4 \text{ eV}$ ³⁷), we can estimate the initial energy of the photofragments, using that in the gas-phase (in the absence of the surrounding ice), the water photofragments (H and OH) have to obey momentum conservation ($p_{\text{H}} = -p_{\text{OH}}$) and energy conservation ($E_{\text{H}} + E_{\text{OH}} = E_{\text{H}_2\text{O}} = E$). The initial available energy E can be calculated from $E = E_{\text{exc}} - E_{\text{diss}}(\text{H}_2\text{O})$, which is in the range of 2.1–4.1 eV depending on the initial excitation energy. The initial energy that the fragments will have can then be estimated according to the following equation:

$$\frac{1}{2}m_{\text{OH}}v_{\text{OH}}^2 = \frac{E}{\left(1 + \frac{m_{\text{OH}}}{m_{\text{H}}}\right)} \quad (3)$$

Therefore, OH radicals will be formed with approximately a maximum translational energy of $E_{\text{OH}} = E/18 = 0.2 \text{ eV}$, and approximately a maximum of vibrational energy E_{v} of 2 eV.²² If the OH is formed with higher vibrational energy, the available total translational energy of OH is reduced by an ‘equal’ amount as follows:

$$E_{\text{OH}}(v) = E_{\text{OH}}(v = 0) - \frac{E_{\text{v}} - E_{v=0}}{18} \quad (4)$$

During the photodissociation dynamics the CO molecule is treated in the same way as the

water molecules that are not photodissociated, i.e., as a rigid rotor. Because the R_{C-O} bond is always fixed to the equilibrium distance of CO the system cannot follow the actual minimum energy path to $H + CO_2$. However, the heights of the barriers change by less than 0.05 eV by fixing $R_{C-O'}$, so that this does not represent a too severe approximation. In line with this, due to its formation process OH may be vibrationally excited initially, and vibrational excitation of OH enhances the gas-phase OH + CO reaction more than vibrational excitation of CO.^{27,44,45} The initial momenta of CO are initialized from a Maxwell Boltzmann distribution of 10 K, and the whole system is equilibrated at the same temperature of 10 K.

For each trajectory only one H_2O molecule is photodissociated and Newtons's equations of motion are integrated using a time step of 0.02 fs and a maximum time t_{max} of 5 ps. The simulation stops if the CO_2 molecule is formed, otherwise all the trajectories are run until t_{max} .

The criterion to define the formation of the CO_2 molecule after the interaction with OH ($OH + CO' \rightarrow CO_2 + H$) is based on the intramolecular distances of $HO-CO'$: $R_{C-O} \leq 1.3 \text{ \AA}$, $R_{C-O'} \leq 1.3 \text{ \AA}$, $R_{O-O'} \leq 3 \text{ \AA}$, and the hydrogen atom originally forming OH is at a distance $R_{O-H} > 2 \text{ \AA}$. The $HOCO'$ complex is defined to be formed if the intramolecular distances are: $R_{H-C} \leq 2.3 \text{ \AA}$, $R_{H-O'} \leq 3.3 \text{ \AA}$, $R_{C-O} \leq 1.5 \text{ \AA}$, $R_{C-O'} \leq 1.3 \text{ \AA}$, and $R_{O-O'} \leq 3 \text{ \AA}$.

Results and discussion

Amorphous ice ball

We considered three different ice balls, and for each of the fourteen closest H_2O molecules to CO between 1000 and 2000 different initial configurations were sampled for each H_2O molecule in the three ice balls taking into account the excitation energies within the first UV absorption band of amorphous water ice.⁴⁶

In our study, three possible outcomes have been observed. We calculated the formation probabilities and its standard errors ($\epsilon = \sqrt{P \cdot (1 - P) / N}$, where P is the probability and N is the total number of trajectories) for these channels for the three different ice balls, which lead to a total number of trajectories of $\approx 48,000$. The predominant outcome channel is the non

reactive one with a probability of 0.970 ± 0.001 , and the second one the formation of the HOCO complex which stays trapped in the ice, with a probability of $(2.98 \pm 1.07) \times 10^{-2}$. The least probable channel is the formation of CO_2 and a hydrogen atom that was always observed to desorb from the ice, with a probability of $(3.6 \pm 0.9) \times 10^{-4}$. The HCO van der Waals complex formation is also observed with an energy of about -18 meV, and a probability of $(2.67 \pm 0.07) \times 10^{-2}$, and this complex always dissociates to CO and H, which desorbs while CO remains trapped inside the ice. The HCO van der Waals complex is defined to be formed if the distance between the H atom formed after H_2O dissociation and the carbon atom from CO $R_{\text{H-C}} \leq 2.1 \text{ \AA}$, and $R_{\text{C-O}}$ is always $< 1.3 \text{ \AA}$ because it is frozen.

CO adsorbed and absorbed in amorphous water ice

We have also studied the formation of CO_2 and HOCO using a set up of amorphous ice similar to the one we have used in earlier MD studies²¹⁻²³ of desorption of H, OH and H_2O from ice following photodissociation of an H_2O molecule in ice. In this Section we discuss an amorphous water ice surface set up at 10 K and a CO molecule that is either adsorbed on top of the first monolayer or located in the second or fifth monolayer (as we described above in the Methods Section). The closest H_2O molecules to the CO molecule were selected to be photoexcited and between 200–2000 different initial conditions were sampled per excited H_2O molecule.

If the CO molecule was initially adsorbed on top of the first monolayer of an amorphous water ice (Fig. 3(a)) no reaction was observed. The final outcome of the 1000 trajectories run in total was that CO stays adsorbed on top of the water ice surface, whereas the H atom always desorbs and the OH fragment either desorbs or stays trapped in the ice, as in our pure water photodissociation results.²¹⁻²³ From the previous calculations on the ice ball system, we conclude that no more than 1000 trajectories were necessary in order to observe some reaction (HOCO that is a prerequisite for the CO_2 formation).

If the CO molecule was initially located in the second monolayer of the amorphous water ice surface (Fig. 3(b)), 2000 trajectories were run in total and only one special event was observed to take place: the HCO van der Waals complex is formed³² –even though we have

used a non reactive HCO PES– for a few femtoseconds (~ 10 fs) after which the complex dissociates to H atom and CO molecule both absorbed in the ice at different locations, and the OH fragment remains trapped in the ice. This channel occurs with a probability of $(3.15 \pm 0.39) \times 10^{-2}$. Watanabe *et al.*¹⁴ also observed HCO experimentally after irradiation of a mixed H₂O–CO ice with UV photons in the range of the Lyman band only for short irradiation times (≤ 10 min). Therefore, the photolysis of a mixed CO–H₂O ice seems to be another possible surface reaction route to HCO formation in interstellar ices. This can be investigated in the future with the use of a reactive H–CO potential.

If the CO molecule was initially located in the fifth monolayer of the amorphous water ice surface (Fig. 3(c)) three different outcomes were observed after running a total of 20,000 trajectories: the non reactive one with a probability of 0.970 ± 0.001 , the formation of the HOCO complex with a probability of $(2.97 \pm 0.12) \times 10^{-2}$, and also the formation of the CO₂ molecule while the H atom desorbs from the ice surface with a probability of $(3.5 \pm 1.3) \times 10^{-4}$. Also in this case the transient formation of the HCO van der Waals complex has been observed, with a probability of $(2.81 \pm 0.12) \times 10^{-2}$.

Therefore, these findings suggest that the initial location of the CO is very important to its subsequent chemistry. If the CO is at the surface or near the surface, a nearby OH photofragment formed upon H₂O photodissociation will usually be in the top two monolayers of the ice surface, and we know from previous MD simulations^{21–23} that these OH fragments tend to desorb to the gas-phase rather than stay trapped in the ice. However, if the OH fragment formed upon H₂O photodissociation was initially located more deeply in the ice it will stay trapped and it is more probable that it will find the right orientation towards the CO molecule to react. The CO molecule and the OH fragment must be located deeply in the water ice system to enable HOCO or CO₂ formation from the reaction with an OH photofragment.

HOCO and CO₂ formation

The most important photoproduct formed in the ice after the reaction of the OH radical with the CO molecule for both types of ice is the HOCO complex, which loses its energy during the dynamics by dissipation to the surrounding H₂O molecules. In these cases, the HOCO

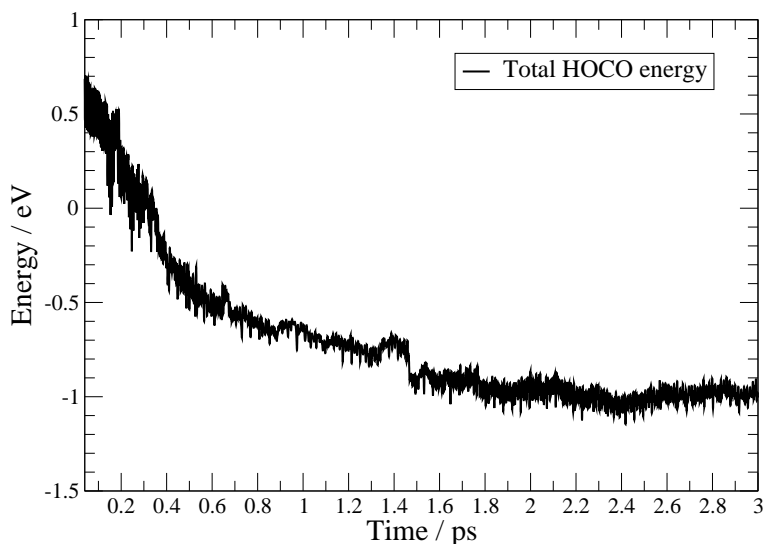


Figure 4: Evolution of the total HOCO energy as a function of time in ps.

complex is trapped in the *trans*-HOCO potential well (see Fig. 1). After enough energy has been transferred to the surrounding ice at 10 K, it becomes nearly impossible to overcome the barriers and form CO₂ and hydrogen, as demonstrated in Fig. 4, where we have plotted the total HOCO energy as a function of the time for one particular trajectory. Fig. 4 shows how fast (in less than 0.2 ps) the HOCO complex may lose its energy, after which it became trapped in the potential well with a total energy of about -1 eV in the case shown (which is close to the *trans*-HOCO minimum energy value, according to the LTSH PES,²⁴ see also Fig. 1).

Goumans *et al.*⁴⁷ already proposed that the reaction between OH and CO may not lead to H + CO₂ when the HOCO complex is formed, because its energy may be dissipated to the surrounding H₂O molecules, after which HOCO can react with atomic H to form CO₂ + H₂, or H₂O and CO, or HCOOH.

The formation of the HOCO complex has been observed by Oba *et al.*¹⁵ in their absorption spectra in both the *trans* and *cis* configurations through peaks at 1812 cm⁻¹ and 1774 cm⁻¹, respectively. These peaks were observed earlier at 1833 cm⁻¹ and 1797 cm⁻¹ by Milligan and Jacox⁴⁸ during vacuum ultraviolet photolysis of H₂O in a CO matrix in the 200–300 nm range. Moreover, Watanabe *et al.*¹³ assumed that the intermediate was formed even though they did not detect it, in order to explain the slow formation rate of CO₂ ice from CO and OH.

In another experiment, Noble *et al.*¹⁷ measured the yield of $^{13}\text{CO}_2$ to be only about 8 % with respect to ^{13}CO . This low yield could be explained assuming that the HOCO intermediate is formed as predicted by gas-phase theoretical^{24,45,49–52} and experimental studies,⁵³ through the reaction of CO with OH. In an ice environment, the reactivity becomes even more complicated than in the gas-phase because it also depends on the initial orientation of the H_2O and CO reactants inside the ice before H_2O is photolysed, and on the resulting orientation of the OH photofragment relative to CO. Francisco *et al.*⁴⁹ studied the stability of the HOCO complex in the gas-phase, and they found that HOCO is stable, in agreement with the far infrared laser magnetic resonance experiment⁵⁴ that confirms that HOCO is stable with a lifetime of about 10 ms. The HOCO complex has two conformers: *trans*-HOCO and *cis*-HOCO. The first one is about 0.1 eV more stable than the second one (Fig. 1). The geometry of both conformers is rather similar: one of the C–O bonds is about 1.34–1.35 Å long, the other one is shorter at 1.18–1.19 Å, and the O–H distance is about 0.97 Å, with 107° – 108° , and 127° – 130° HOC, and OCO bond angles, respectively.^{45,49,50}

According to our simulations and taking into account the two types of ice, the probability to form the HOCO complex is $(3.00 \pm 0.07) \times 10^{-2}$. On average the HOCO complex that is observed trapped in the ices has the following geometry: one of the C–O bonds is about 1.37 Å long, and the other CO distance corresponding to the original CO molecule is always kept fixed, because in our simulations the CO is treated as a rigid rotor, at a bond length of 1.13 Å. The O–H distance is about 0.91 Å, the HOC angle is about 120° – 136° , this range being somewhat larger than in the gas-phase, the OCO bond angle is about 123° on average, which is close to the gas-phase value, and the dihedral HO–CO angle is on average 175° . Therefore, the HOCO complex that is observed as trapped in the ice matrix has a geometry close to the *trans*-HOCO complex,^{45,50} and its energy (see Fig. 4) agrees with the minimum of the *trans*-HOCO complex in the LTSH potential²⁴ used (see Fig. 1). The fixed CO bond distance in our simulations does not affect the minimum reaction barrier height relative to the gas-phase reactants (i.e., with this approximation the exit channel barrier height is only 0.02 eV higher).

The total calculated probability to form $\text{CO}_2 + \text{H}$ for the two kinds of ice investigated is $(3.6 \pm 0.7) \times 10^{-4}$, which is very low and the reaction only occurs when the initial excitation energy

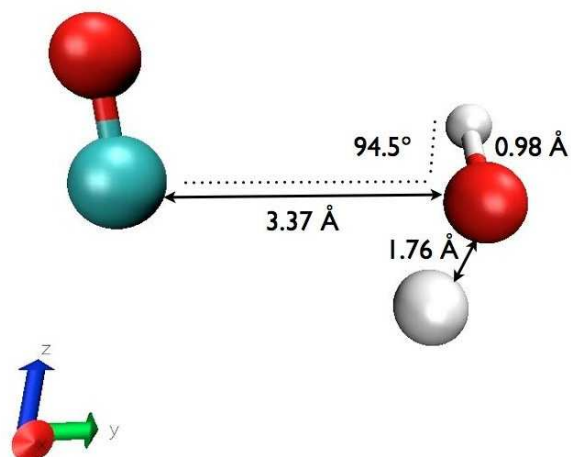


Figure 5: Initial configuration of CO and OH after H₂O photodissociation that leads to the formation of CO₂. Red balls represent O, white H, and green C atoms.

of the photoexcited water molecule is on average (8.83 ± 0.23) eV. At these energies usually vibrationally excited OH is produced on average at $\nu=1$ with a vibrational energy $E_v \approx 0.7$ eV. We analyzed the initial configurations and orientations of the reactant molecules that lead to CO₂ and the main conclusions are that the initial distance between the C atom from CO and the oxygen atom from the reacting OH fragment has to be within the range $3.1 \text{ \AA} \leq R_{\text{CO}} \leq 3.5 \text{ \AA}$, and the dihedral angle between the OH bond and CO bond has to be in the range $41^\circ - 178^\circ$ as is illustrated in Fig. 5 where the angle is 94.5° . During the dynamics OH approaches CO and orientates itself in a *trans* conformation relative to CO, and in less than 0.05 ps and without going through the *cis*-HOCO conformation the OH bond breaks and CO₂ and H are formed.

We compared the probability to form CO₂ in the ice with gas-phase calculations performed using the VENUS96 code⁵⁵ and using the LTSH PES²⁴ implemented as described in Ref.²⁶ The collision energy of OH was set to 0.17 eV, which corresponds to the initial energy OH fragments would have on average in the ice if the water molecules were initially excited with an energy of 8.6 eV (corresponding to the peak of the first UV absorption band of amorphous water ice⁴⁶), and the impact parameter range was between 0 and 2.4 Å.

Fig. 6 presents the fitted reaction probability as a function of impact parameter for four

values of ν . For each value of ν , the initial available total translational energy of OH is calculated according to Eq. 4 (e.g., for $\nu=0, 1, 2$, and 3 , $E_{\text{OH}}(\nu)=0.17, 0.15, 0.13$, and 0.11 eV, respectively). From Fig. 6 it is clear that increasing the vibrational energy of the reactants increases the reaction probability as well even though the translational energy of OH is reduced, in agreement with very recent theoretical gas-phase calculations⁴⁴ where a full-dimensional time-dependent wave packet study based on the LTSH potential²⁴ showed how the reactivity is enhanced by initial OH vibrational excitation. The probabilities to form CO₂ in the gas-phase for OH in $\nu=0, 1, 2$, and 3 are $0.01, 0.037, 0.063$, and 0.082 , respectively at $b=0$ Å (Fig. 6). The most reactive trajectories are those that start with the OH radical more or less in line with the CO molecule, O of OH closes to C of CO. Therefore, in the gas-phase the probability to form CO₂ and hydrogen from OH + CO is higher than in our calculations. But these probabilities are for impact parameter $b=0$ Å, and they decrease when the impact parameter increases up to a maximum impact parameter of about 2 Å (Fig. 6), whereas in our simulations when water dissociates in ice into OH and H, the OH radical collides with CO at different impact parameters. In particular, the calculated impact parameter b for the reactive trajectories was within the range $1.27\text{--}4.4$ Å, on average being (2.94 ± 0.86) Å. Moreover, in the solid state the environment is also completely different than in the gas-phase because the OH and the CO molecules also interact with the other H₂O molecules in the ice and they may release their energy to the environment, which may also decrease the reactivity.

We have analyzed our simulations for the two types of ice systems and found that initially the OH vibrational state distributions mostly correspond to $\nu=0, 1, 2$, and 3 , using box quantization to assign vibrational states with inclusion of zero-point energy. The OH vibrational energy distribution agrees with the experimental gas-phase distribution⁵⁶ for H₂O photodissociation at 7.9 eV (this value was chosen because the production of OH in ice is shifted by the same amount as the absorption spectrum). The experimental data show that when H₂O dissociates several vibrational states are assigned to the OH photoproduct with $\nu=0, 1, 2, 3$, and 4 .

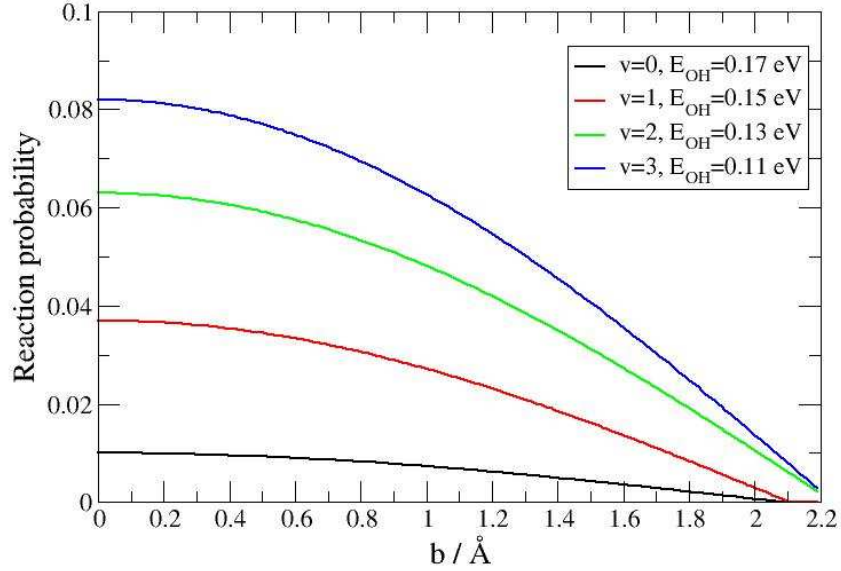


Figure 6: Gas-phase fitted reaction probability on the LTSH PES²⁴ versus the impact parameter at $v=0, 1, 2,$ and 3 .

Comparison with the experiments

The comparison with the experiments that study the formation of CO₂ ice through the reaction of CO with OH, where the OH comes from UV dissociation of H₂O ice,^{13,14} is not straightforward. The experiments only provide the rates to convert CO into CO₂ based on the variation of the column densities as a function of irradiation time, and from these data a first-order rate equation law is fit. On the other hand, from our theoretical models we can provide the formation probabilities of CO₂ and HOCO in ice per absorbed UV photon, which are $(3.6 \pm 0.7) \times 10^{-4}$, and $(3.00 \pm 0.07) \times 10^{-2}$ (Table 1), respectively, where it is assumed that, as in the gas-phase photoabsorption, each absorbed photon leads to dissociation into H and OH.

In order to estimate the same probability from the experiments performed by Watanabe *et al.*,¹³ we need, besides the photon flux used in the experiments, the number of water and CO molecules in the sample, and the photon absorption cross section (σ) of amorphous ice in the Ly α (10.21 eV) region. Unfortunately, σ is not accurately known. Ref.⁵⁷ claims it to be close to the absorption coefficient of liquid water and around 30% of the gas-phase value.

Accurate values of the gas-phase cross section are given in Ref.⁵⁸ at exactly Ly α and in Ref.⁵⁹ for the whole VUV range. Here we use a gas-phase cross section, σ_{gas} , averaged over the 116–136 nm range used in the experiment,⁵⁹ $\sigma_{\text{gas}}=7.1 \times 10^{-18} \text{ cm}^2$. Let I_0 be the experimental photon flux per cm^2 per second. Then the number of photons absorbed per second per cm^2 follows from Beer's law as:

$$I_0 - I = I_0(1 - e^{-\sigma \cdot n \cdot l}) \quad (5)$$

where n is the number density (in cm^{-3}) of H_2O molecules in the sample and l the optical path length, which is twice the sample thickness because the light is reflected at the sample support.

The number density of H_2O can be computed from the density d of amorphous ice (0.94 g cm^{-3})⁶⁰ taking into account that a 1 to 10 mixture of CO and H_2O contains 91% H_2O , so that $n=N_{\text{av}} \cdot d \cdot 0.91/m_{\text{H}_2\text{O}}$, where $m_{\text{H}_2\text{O}}$ is the molar mass of H_2O . Noting that the mixing ratio used is 10, we make the approximation that any H_2O molecule in the experimental sample that is photodissociated will be close to one CO molecule with which it can react, as in our model. Errors due to this approximation are not likely to exceed a factor 2.

In Watanabe's experiment,¹³ the measured photon flux is $I_0=9.2 \times 10^{13} \text{ photons s}^{-1} \text{ cm}^{-2}$, and the estimated double path length is $l=1.6 \times 10^{-6} \text{ cm}$. Thus, applying Eq. 5 the probability that a UV photon will be absorbed in the experiments should be about 0.28, and per second the number of OH radicals formed in the experimental ice sample ($l=1.6 \times 10^{-6} \text{ cm}$) per surface area of 1 cm^2 should be $2.3 \times 10^{13} (N_{\text{OH}})$, which may react with CO molecules. The number of CO molecules (N_{CO}) in a sample of $0.8 \times 10^{-6} \text{ cm}$ is equal to¹³ $N_{\text{CO}}=0.1 \cdot n \cdot 0.8 \times 10^{-6} = 2.32 \times 10^{15}$.

Watanabe *et al.*¹³ measured the time variation of the integrated absorbance of CO molecules with respect to the initial amount of CO molecules (see figure 3 in Ref.¹³) and also the time variation of integrated absorbance of CO_2 normalized to the initial integrated absorbance of CO (see figure 4 in Ref.¹³). From the fits of the two curve (figures 3 and 4 in Ref.¹³) they obtained rate constants equal to $6.5 \times 10^{-4} \text{ s}^{-1}$, and $2.5 \times 10^{-4} \text{ s}^{-1}$ for the time destruction of CO and formation of CO_2 , respectively. From the CO destruction rate $6.5 \times 10^{-4} \text{ s}^{-1}$, we derive that per

second 1.5×10^{12} CO molecules are converted, either to form HOCO or CO₂. Summarizing, in the experiment for each OH formed, $1.5 \times 10^{12} / 2.3 \times 10^{13} = 0.07$ molecule CO disappears. This number is significantly larger than the value obtained in the simulations $(3.6 \pm 0.7) \times 10^{-4}$. On the other hand, the experimentalists concluded that if CO converts immediately to CO₂ both rate constants should be the same, but they are not. Therefore, in their experiments there must be some intermediate in the solid state before CO₂ is formed. This intermediate could be the HOCO complex even though it was not observed in their FTIR measurements.

In our simulations, the probability to destroy CO and form CO₂ is much lower than the experimental value, if we assume that in the experiments all destroyed CO molecules correspond to CO₂ formation (see Table 1). However, our results suggest that the HOCO complex is formed in the ice and that it is stabilized by energy dissipation. Therefore, if we compare the total calculated probability (Table 1) to form HOCO and CO₂ with the experimental value assuming that all the CO that is destroyed results into HOCO or CO₂ the agreement is rather good, even though there was no experimental evidence for large HOCO concentrations inside the ice in this particular experiment. But in a later experiment Watanabe *et al.*¹⁴ found two peaks at 1808 and 1784 cm⁻¹ that they decided not to investigate. However, we believe that these two peaks correspond to the *trans*-HOCO and *cis*-HOCO complex with frequencies of 1774 cm⁻¹ and 1812 cm⁻¹, respectively according to Oba *et al.*,¹⁵ and 1797 cm⁻¹, and 1833 cm⁻¹ (measured in a matrix), respectively, according to Milligan & Jacox.⁴⁸ Thus, it is possible that these features were also present in the earlier experiments of Watanabe *et al.*¹³ but not reported.

A large difference between the theory and the experiments is that in the theory only one CO molecule and one nearby H₂O molecule excited by a single photon are considered, whereas in

Table 1: Experimental¹³ and theoretical probabilities after CO and OH reaction in the ice.

Channel	Experim. probability ¹³	Theoret. probability (this work)
Total CO conversion	7.00×10^{-2}	$(3.01 \pm 0.07) \times 10^{-2}$
CO ₂ and H formation	2.69×10^{-2}	$(3.6 \pm 0.7) \times 10^{-4}$
HOCO formation	-	$(3.0 \pm 0.1) \times 10^{-2}$

the laboratory conditions several OH radicals are produced that can interact with several CO molecules, and find the ideal orientation and react. Another important difference is that in our theoretical study we excite H₂O molecules to the first excited state (\tilde{A}^1B_1) leading to H and OH, with the OH radical in its electronic ground state (X). However, in the experiments the ice is irradiated with photons with energies close to the Ly α energy, which includes absorption into the \tilde{B}^1A_1 state and may lead to the formation of: OH(X) + H, OH(A) + H, O(3P) + 2H, and O(1D) + H₂, with the corresponding experimental branching ratios of: 0.64, 0.14, 0.22, and 0, respectively, according to Mordaunt *et al.*⁶¹ It is also known from gas-phase experiments⁶² and theoretical calculations⁶³ that the OH(X) product has a vibrational state distribution mostly only populated at $v=0$, whereas the OH(A) product after H₂O photodissociation at Ly α is formed not only in $v=0$, but also in $v=1$ and 2 in the gas-phase. Since the OH(X) radicals in $v=0$ are not so reactive (Fig. 6), the OH radicals in the excited state (A) may well be responsible for the reaction with CO in the experiments.

Improvements of the model

In our previous studies^{21,22} we already discussed the most important approximations introduced in the study of molecular dynamics simulations of water ice photodissociation. Here, we discuss the ones that may effect our results regarding the formation of CO₂ through the reaction of CO with OH formed upon H₂O photodissociation. We list them as follows:

1. The formation of CO₂ ice has been studied only through the CO + OH(X) route. The photoexcitation of H₂O to the first electronic excited state only leads to OH(X) molecule in its ground state and H atom. In the experiments H₂O can also be photoexcited to the second excited electronic state and its dissociation can lead to the formation of OH(X) + H, OH(A) + H, O(3P) + 2H, and O(1D) + H. In principle, two additional routes may then lead to the formation of CO₂: (1) CO + O(3P) \rightarrow CO₂, which can also take place when the O(3P) is formed after the reaction of two OH radicals formed upon independent H₂O dissociation processes, (2) CO + OH(A) \rightarrow CO₂ + H, which probably has a higher associated reaction probability than the CO + OH(X) reaction, as we already discussed in

the previous section. Therefore, a more precise comparison with the experiments could be enabled by also modeling the excitation of H₂O to the \tilde{B} state in our simulations. Also, experiments could be carried out in which H₂O ice is irradiated at lower excitation energies, so that only excitation to the \tilde{A} state is possible, which would enable a better comparison to the present theoretical work. Another difference with the experiments is the CO/H₂O ratio being equal to 10 which is much larger than in our model. Therefore, in the experimental ice sample, the H₂O molecules can probably rotate more easily and eventually find the best orientation to react with CO. On the other hand, our model is well suited to the description of interstellar chemistry in terms of photon fluxes (which are very low, meaning that the photodissociation by one incident photon is completely finished by the time the next photon arrives). But with the interstellar radiation field, excitation should also be possible to the \tilde{B} state of H₂O.

2. The particular HOCO PES used in the model may introduce some errors in the reactivity. The HOCO PES that we considered is the LTSH PES.²⁴ Gas-phase calculations⁴⁵ computed for the HO + CO reaction by means of different PESs showed differences in the cross sections obtained, but only at collision energies $E_c > 0.65$ eV (15 kcal/mol). However, for the collision energies we are considering ($E_c < 0.17$ eV (3.9 kcal/mol)) the differences in the cross sections obtained with different PESs are almost negligible (see Fig.4(a) in Ref.⁴⁵).
3. Not including quantum effects may be important at the low temperatures here considered. However, in the gas-phase calculations⁴⁵ quantum effects are small, therefore we assume they will also be small in the solid state environment considered here.
4. In our model we have treated the interaction between H and CO through a non reactive HCO PES. Thus, no competition with HCO formation has been introduced, and in the future we are planning to also include a reactive HCO PES in order to quantify the probability of HCO ice formation in the interstellar medium. It should be noted that HCO formation would probably occur at the cost of the CO₂ formation.

Summary and Conclusions

Molecular dynamics simulations have been performed for two different CO–H₂O ice systems in order to study the formation of CO₂ in interstellar ices upon irradiation with UV photons. After the absorption of an UV photon H₂O dissociates into H and OH, and the OH radical can react with the CO present in the ice and form CO₂.

The first type of ice is based on the ‘hit and stick’ method with a single CO molecule in the center and 50 water molecules around it yielding an ice ball. Three different initial ice balls were set up at 10 K and several H₂O molecules were chosen to be photodissociated. We calculated the probabilities to form the HOCO complex and the CO₂ molecule, and also the probability to form the transient HCO van der Waals complex.

The second kind of ice was based on our previous MD simulations of amorphous water ice dissociation,^{21–23} and by using the same procedure an amorphous water ice at 10 K was set up with either a CO molecule adsorbed on the topmost ML or located in the second or fifth monolayer. Several initial conditions were sampled for the three cases, and no reaction was observed in the first case (CO_{ad} adsorbed on the surface). In the second case (CO_{ab} in ML 2) only the formation of the HCO van der Waals complex was registered (even though a non reactive HCO PES was used), and in the end this resulted in the H atom desorbing from the ice and the CO molecule being trapped inside the ice. However, if the CO was initially absorbed in ML 5, the HOCO complex and the CO₂ molecule can be formed and the probabilities of these events were calculated.

The formation of the HOCO complex is much more probable than the formation of CO₂, because once the HOCO complex is formed it immediately starts losing its internal energy and it may become trapped inside the ice matrix. The HOCO complex has been detected experimentally by Oba *et al.*,¹⁵ and Watanabe *et al.*¹³ also claimed that this complex must be formed as an intermediate that in the end may dissociate into CO₂ and hydrogen atom. The comparison with the experiments is not straightforward mostly because the experimentalists irradiate the ice with a broadlamp peaking near Ly α , exciting the water molecules to the higher excited \tilde{B} state. We have deduced from their data the number of photons that lead to conversion

of CO into HOCO or further to CO₂ after irradiating the CO–H₂O mixed ice with UV photons close to Ly α energies. If we assume that all the CO is converted into CO₂ in the experiments, the experimental probability is much higher than our probability to form CO₂. However, if we assume that CO can be converted to HOCO and/or CO₂, our total probability to form both molecules agrees reasonably well with their value.

Overall, we can summarize the conclusions as follows:

1. The initial location of the CO molecule in the ice surface is very important as found from both types of ice simulated. This means that not only the environment (e.g., the number of nearest neighbor water molecules and their orientations relative to CO), but also the initial position of the CO molecule plays a big role. The CO must be located deep in the ice system. In conclusion, it is the initial position of the CO molecule and not the type of ice we modeled that appears to affect the reactivity of the OH photofragment with CO.
2. CO₂ ice can be formed through the OH + CO reaction where the OH comes from H₂O photodissociation, if the water molecule has been excited with energies higher than 8.6 eV. However, the HOCO complex is the main product in our simulations.
3. HCO ice can probably also be formed through the H + CO reaction where the H comes from H₂O photodissociation.
4. Experiments regarding the OH + CO reaction upon excitation of H₂O in the first absorption band of amorphous water ice are necessary in order to confirm our theoretical results. If H₂O is excited in the second absorption band (as has been done in all existing experiments) other channels besides the OH(X) + H are possible after H₂O dissociation, and even the OH(X) formed will likely have a different reactivity with CO, due to a higher initial vibrational energy content.
5. A new theoretical model able to photoexcite H₂O to be \tilde{B} state is needed in order to explore other possible routes to form CO₂ ice.

Acknowledgement

The authors would like to thank S. Andersson for providing the *ab initio* data and the fitting of some of the potential energy surfaces employed in our model, and R. Valero for providing the implemented LTSH PES in the VENUS code. This project was funded with computer time by NCF/NWO, and by NWO astrochemistry grant No. 648.000.010.

Supporting Information Available

The parameters of the pair potentials and its analytical expressions, the analytical expressions of the switching functions, and the operational definition of the outcome products (5 pages).

References

- (1) Tielens, A. G. G. M.; Tokunaga, A. T.; Geballe, T. R.; Baas, F. Interstellar solid CO - Polar and nonpolar interstellar ices. *Astrophys. J.* **1991**, *381*, 181–199.
- (2) Boogert, A. C. A.; Pontoppidan, K. M.; Knez, C.; Lahuis, F.; Kessler-Silacci, J.; van Dishoeck, E. F.; Blake, G. A.; Augereau, J.-C.; Bisschop, S. E.; Bottinelli, S. *et al.* The c2d Spitzer Spectroscopic Survey of Ices around Low-Mass Young Stellar Objects. I. H₂O and the 5–8 μ m Bands. *Astrophys. J.* **2008**, *678*, 985 – 1004.
- (3) d’Hendecourt, L. B.; de Muizon, M. J. The discovery of interstellar carbon dioxide. *Astron. Astrophys.* **1989**, *223*, L5–L8.
- (4) de Graauw, T.; Whittet, D. C. B.; Gerakines, P. A.; Bauer, O. H.; Beintema, D. A.; Boogert, A. C. A.; Boxhoorn, D. R.; Chiar, J. E.; Ehrenfreund, P.; Feuchtgruber, H. *et al.* SWS observations of solid CO₂ in molecular clouds. *Astron. Astrophys.* **1996**, *315*, L345–L348.
- (5) Pontoppidan, K. M.; Boogert, A. C. A.; Fraser, H. J.; van Dishoeck, E. F.; Blake, G. A.; Lahuis, F.; Öberg, K. I.; Evans, I., N. J.; Salyk, C. The c2d Spitzer Spectroscopic Survey of Ices around Low-Mass Young Stellar Objects. II. CO₂. *Astrophys. J.* **2008**, *678*, 1005–1031.
- (6) Hasegawa, T. I.; Herbst, E.; Leung, C. M. Models of gas-grain chemistry in dense interstellar clouds with complex organic molecules. *Astrophys. J. Sup. Series* **1992**, *82*, 167–195.
- (7) Gibb, E. L.; Whittet, D. C. B.; Boogert, A. C. A.; Tielens, A. G. G. M. Interstellar Ice: The Infrared Space Observatory Legacy. *Astrophys. J. Sup. Series* **2004**, *151*, 35–73.
- (8) Loeffler, M. J.; Baratta, G. A.; Palumbo, M. E.; Strazzulla, G.; Baragiola, R. A. CO₂ synthesis in solid CO by Lyman- α photons and 200 keV protons. *Astron. Astrophys.* **2005**, *435*, 587–594.

- (9) Jamieson, C. S.; Mebel, A. M.; Kaiser, R. I. Understanding the Kinetics and Dynamics of Radiation-induced Reaction Pathways in Carbon Monoxide Ice at 10 K. *Astrophys. J. Sup. Series* **2006**, *163*, 184–206.
- (10) Bennett, C. J.; Jamieson, C. S.; Kaiser, R. I. Mechanistical studies on the formation of carbon dioxide in extraterrestrial carbon monoxide ice analog samples. *Phys. Chem. Chem. Phys.* **2009**, *11*, 4210–4218.
- (11) Roser, J. E.; Vidali, G.; Manicó, G.; Pirronello, V. Formation of Carbon Dioxide by Surface Reactions on Ices in the Interstellar Medium. *Astrophys. J.* **2001**, *555*, L61–L64.
- (12) Madzunkov, S.; Shortt, B. J.; MacAskill, J. A.; Darrach, M. R.; Chutjian, A. Measurements of polyatomic molecule formation on an icy grain analog using fast atoms. *Phys. Rev. A* **2006**, *73*, 020091–1–020091–4.
- (13) Watanabe, N.; Kouchi, A. Measurements of Conversion Rates of CO to CO₂ in Ultraviolet-induced Reaction of D₂O(H₂O)/CO Amorphous Ice. *Astrophys. J.* **2002**, *567*, 651–655.
- (14) Watanabe, N.; Mouri, O.; Nagaoka, A.; Chigal, T.; Kouchi, A.; Pirronello, V. Laboratory Simulation of Competition between Hydrogenation and Photolysis in the Chemical Evolution of H₂O-CO Ice Mixtures. *Astrophys. J.* **2007**, *668*, 1001–1011.
- (15) Oba, Y.; Watanabe, N.; Kouchi, A.; Hama, T.; Pirronello, V. Experimental Study of CO₂ Formation by Surface Reactions of Non-energetic OH Radicals with CO Molecules. *Astrophys. J. Lett.* **2010**, *712*, L174–L178.
- (16) Ioppolo, S.; van Boheemen, Y.; Cuppen, H. M.; van Dishoeck, E. F.; Linnartz, H. Surface formation of CO₂ ice at low temperatures. *Mon. Not. R. Astron. Soc.* **2011**, *413*, 2281–2287.
- (17) Noble, J. A.; Dulieu, F.; Congiu, E.; Fraser, H. J. CO₂ Formation in Quiescent Clouds: An Experimental Study of the CO + OH Pathway. *Astrophys. J.* **2011**, *735*, 121–1–121–6

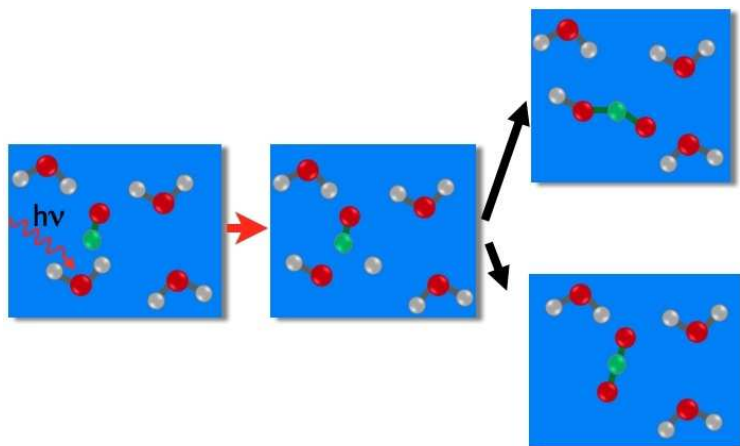
- (18) Zins, E.-L.; Joshi, P. R.; Krim, L. Reactivity between a CO-containing Ice and Non-energetic OH Radicals. *Astrophys. J.* **2011**, *738*, 175–1–175–7.
- (19) Grim, R. J. A.; d'Hendecourt, L. B. Time-dependent chemistry in dense molecular clouds. IV - Interstellar grain surface reactions inferred from a matrix isolation study. *Astron. Astrophys.* **1986**, *167*, 161–165.
- (20) Talbi, D.; Chandler, G. S.; Rohl, A. L. The interstellar gas-phase formation of CO₂ Assisted or not by water molecules? *Chem. Phys.* **2006**, *320*, 214–228.
- (21) Andersson, S.; Al-Halabi, A.; Kroes, G.-J.; van Dishoeck, E. F. Molecular-dynamics study of photodissociation of water in crystalline and amorphous ices. *J. Chem. Phys.* **2006**, *124*, 064715–1–064715–14
- (22) Andersson, S.; van Dishoeck, E. F. Photodesorption of water ice. A molecular dynamics study. *Astron. Astrophys.* **2008**, *491*, 907–916.
- (23) Arasa, C.; Andersson, S.; Cuppen, H. M.; van Dishoeck, E. F.; Kroes, G.-J. Molecular dynamics simulations of the ice temperature dependence of water ice photodesorption. *J. Chem. Phys.* **2010**, *132*, 184510–1–184510–12.
- (24) Lakin, M. J.; Troya, D.; Schatz, S.; Harding, L. B. A quasiclassical trajectory study of the reaction $\text{OH} + \text{CO} \rightarrow \text{H} + \text{CO}_2$. *J. Chem. Phys.* **2003**, *119*, 5848–5859.
- (25) McCormack, D. A.; Kroes, G. J. Converged five-dimensional quantum calculations for $\text{OH} + \text{CO} \rightarrow \text{H} + \text{CO}_2$. *J. Chem. Phys.* **2002**, *116*, 4184–4191.
- (26) Valero, R.; van Hemert, M. C.; Kroes, G. J. Classical trajectory study of the HOCO system using a new interpolated ab initio potential energy surface. *Chem. Phys. Lett.* **2004**, *393*, 236–244.
- (27) Valero, R.; McCormack, D. A.; Kroes, G. J. New results for the $\text{OH} (v=0, j=0) + \text{CO} (v=0, j=0) \rightarrow \text{H} + \text{CO}_2$ reaction: Five- and full-dimensional quantum dynamical study on several potential energy surfaces. *J. Chem. Phys.* **2004**, *120*, 4263–4272.

- (28) Herbst, E.; van Dishoeck, E. F. Complex Organic Interstellar Molecules. *Annu. Rev. Astron. Astrophys.* **2009**, *47*, 427–480.
- (29) Ehrenfreund, P.; Fraser, H. *Solid State Astrochemistry*, V. Pirronello, J. Krelowski (Eds.); Kluwer Academic Publishers: Dordrecht, 2003; p 317.
- (30) Garrod, R. T.; Herbst, E. Formation of methyl formate and other organic species in the warm-up phase of hot molecular cores. *Astron. Astrophys.* **2006**, *457*, 927–936.
- (31) Allen, M. P.; Tildesley, D. J. *Computer Simulations of Liquids*; Clarendon: Oxford, 1987.
- (32) Arasa, C.; van Hemert, M. C.; van Dishoeck, E. F.; Kroes, G. J. This material is available via the Internet at. <http://pubs.acs.org/>.
- (33) Jorgensen, W. L.; Chandrasekhar, J.; Madura, J. D.; Impey, R. W.; Klein, M. L. Comparison of simple potential functions for simulating liquid water. *J. Chem. Phys.* **1983**, *79*, 926–935.
- (34) Kroes, G.-J.; Clary, D. C. Sticking of HCl and ClOH to ice: A Computational Study. *J. Phys. Chem.* **1992**, *96*, 7079–7088.
- (35) Dobbyn, A. J.; Knowles, P. J. A comparative study of methods for describing non-adiabatic coupling: diabatic representation of the $^1\Sigma + / ^1\Pi$ HOH and HHO conical intersections. *Mol. Phys.* **1997**, *91*, 1107–1123.
- (36) Aoiz, F. J.; Bañares, L.; Castillo, J. F.; Brouard, M.; Denzer, W.; Vallance, C.; Honvault, P.; Launay, J.-M.; Dobbyn, A. J.; Knowles, P. J. Insertion and Abstraction Pathways in the Reaction $O(^1D_2) + H_2 \rightarrow OH + H$. *Phys. Rev. Lett.* **2001**, *86*, 1729–1732.
- (37) van Harrevelt, R.; van Hemert, M. C. Photodissociation of water in the \tilde{A} band revisited with new potential energy surfaces *J. Chem. Phys.* **2001**, *114*, 9453–9462.
- (38) Murty, K. G. *Linear programming*; John Wiley & Sons Inc.: New York, 1983.

- (39) Berendsen, H. J. C.; Postma, J. P. M.; van Gunsteren, W. F.; DiNola, A.; Haak, J. R. Molecular dynamics with coupling to an external bath. *J. Chem. Phys.* **1984**, *81*, 3684–3690.
- (40) Al-Halabi, A.; van Dishoeck, E. F.; Kroes, G.-J. Sticking of CO to crystalline and amorphous ice surfaces. *J. Chem. Phys.* **2004**, *120*, 3358–3367.
- (41) Al-Halabi, A.; Fraser, H. F.; Kroes, G.-J.; van Dishoeck, E. F. Adsorption of CO on amorphous water-ice surfaces. *Astron. Astrophys.* **2004**, *422*, 777–791.
- (42) van Harrevelt, R.; van Hemert, M. C.; Schatz, G. C. A Comparative Classical-Quantum Study of the Photodissociation of Water in the \tilde{B} Band. *J. Phys. Chem. A* **2001**, *105*, 11480–11487.
- (43) Schinke, R. *Photodissociation Dynamics*; Cambridge University Press: Cambridge, 1993.
- (44) Liu, S.; Xu, X.; Zhang, D. H. A full dimensional time-dependent wave packet study of the $\text{OH} + \text{CO} \rightarrow \text{H} + \text{CO}_2$ reaction. *Theor. Chem. Acc.* **2012**, *131*, 1068–1–1068–7.
- (45) Li, J.; Xie, C.; Ma, J.; Wang, Y.; Dawes, R.; Xie, D.; Bowman, J. M.; Guo, H. Quasi-Classical Trajectory Study of the $\text{HO} + \text{CO} \rightarrow \text{H} + \text{CO}_2$ Reaction on a New ab Initio Based Potential Energy Surface. *J. Phys. Chem. A* **2012**, *116*, 5057–5067.
- (46) Kobayashi, K. Optical Spectra and Structure of Ice. *J. Chem. Phys.* **1983**, *87*, 4317–4321.
- (47) Goumans, T. P. M.; Uppal, M. A.; Brown, W. A. Formation of CO_2 on a carbonaceous surface: a quantum chemical study. *Mon. Not. R. Astron. Soc.* **2008**, *384*, 1158–1164.
- (48) Milligan, D. E.; Jacox, M. E. Infrared Spectrum and Structure of Intermediates in the Reaction of OH with CO. *J. Chem. Phys.* **1971**, *54*, 927–942.
- (49) Francisco, J. S.; Muckerman, J. T.; Yu, H.-G. HOCO Radical Chemistry. *Acc. Chem. Rev.* **2010**, *43*, 1519–1526.

- (50) Li, J.; Wang, Y.; Jiang, B.; Ma, J.; Dawes, R.; Xie, D.; Bowman, J. M.; Guo, H. Communication: A chemically accurate global potential energy surface for the $\text{HO} + \text{CO} \rightarrow \text{H} + \text{CO}_2$. *J. Chem. Phys.* **2012**, *136*, 041103–1–041103–4.
- (51) Song, X.; Li, J.; Hou, H.; Wang, B. Ab initio study of the potential energy surface for the $\text{OH} + \text{CO} \rightarrow \text{H} + \text{CO}_2$ reaction. *J. Chem. Phys.* **2006**, *125*, 094301–1–094301–6.
- (52) Yu, H.-G.; Muckerman, J. T.; Sears, T. J. A theoretical study of the potential energy surface for the reaction $\text{OH} + \text{CO} \rightarrow \text{H} + \text{CO}_2$. *Chem. Phys. Lett.* **2001**, *349*, 547–554.
- (53) Alagia, M.; Balucani, N.; Casavecchia, P.; Stranges, D.; Volpi, G. G. Crossed beam studies of fouratom reactions: The dynamics of $\text{OH} + \text{CO}$. *J. Chem. Phys.* **1993**, *98*, 8341–8344.
- (54) Sears, T. J.; Radford, H. E.; Moore, M. A. *b*-dipole transitions in *trans*-HOCO observed by far infrared laser magnetic resonance. *J. Chem. Phys.* **1993**, *98*, 6624–6631.
- (55) Hase, W. L.; Duchovic, R. J.; Hu, X.; Komornicki, A.; Lim, K. F.; Lu, D. h.; Peshherbe, G. H.; Swamy, K. N.; Vande Linde, S. R.; Varandas, A. *et al.* *VENUS96: A General Chemical Dynamics Computer Program, Quantum Chemistry Program Exchange* **1996**, *16*, 671.
- (56) Hwang, D. W.; Yang, X.; Yang, X. The vibrational distribution of the OH product from H_2O photodissociation at 157 nm: Discrepancies between theory and experiment. *J. Chem. Phys.* **1999**, *110*, 4119–4126.
- (57) Hayashi, H.; Watanabe, N.; Udagawa, Y.; Kao, C.-C. The complete optical spectrum of liquid water measured by inelastic x-ray scattering. *Proc. Natl. Acad. Sci. U.S.A.* **2000**, *97*, 6264–6266.
- (58) Vatsa, R. K.; Volpp, H.-R. Absorption cross-sections for some atmospherically important molecules at the H atom Lyman- α wavelength (121.567 nm). *Chem. Phys. Lett.* **2001**, *340*, 289–295.

- (59) Cheng, B.-M.; Chung, C.-Y.; Bahou, M.; Lee, Y.-P.; Lee, L. C.; van Harrevelt, R.; van Hemert, M. C. Quantitative spectroscopic and theoretical study of the optical absorption spectra of H₂O, HOD, and D₂O in the 125-145 nm region. *J. Chem. Phys.* **2004**, *120*, 224–229.
- (60) Murray, B. J.; Jensen, E. J. Homogeneous nucleation of amorphous solid water particles in the upper mesosphere. *J. Atm. Sol-Terr. Phys.* **2000**, *72*, 51–61.
- (61) Mordaunt, D. H.; Ashfold, M. N. R.; Dixon, R. N. Dissociation dynamics of H₂O(D₂O) following photoexcitation at the Lyman- α wavelength (121.6 nm). *J. Chem. Phys.* **1994**, *100*, 7360–7375.
- (62) Harich, S. A.; Hwang, D. W. H.; Yang, X.; Lin, J. J.; Yang, X.; Dixon, R. N. Photodissociation of H₂O at 121.6 nm: A state-to-state dynamical picture. *J. Chem. Phys.* **2000**, *113*, 10073–10090.
- (63) Fillion, J. H.; van Harrevelt, R.; Ruiz, J.; Castillejo, M.; Zanganeh, A. H.; Lemaire, J. L.; van Hemert, M. C.; Rostas, F. Photodissociation of H₂O and D₂O in \tilde{B} , \tilde{C} , and \tilde{D} States (134 - 119 nm). Comparison between Experiment and ab Initio Calculations. *J. Phys. Chem. A* **2001**, *105*, 11414–11424.



This material is available free of charge via the Internet at <http://pubs.acs.org/>.